



1 **Dynamic changes of terrestrial net primary production and its** 2 **feedback to evapotranspiration**

3 Zhi Li¹, Yaning Chen¹, Yang Wang² and Gonghuan Fang^{1,3}

4 ¹State Key Laboratory of Desert and Oasis Ecology, Xinjiang Institute of Ecology and Geography, Chinese Academy of
5 Sciences, Urumqi 830011, China

6 ²College of Pratacultural and Environmental Sciences, Xinjiang Agricultural University, Urumqi 830052, China

7 ³Department of Geography, Ghent University, Ghent, Belgium

8 *Correspondence to:* Yaning Chen (chenyn@ms.xjb.ac.cn)

9 **Abstract.** Earth experienced dramatic environmental changes in the recent 15 years (2000-2014). The
10 past decade has been the warmest in the instrumental record, which significantly influences the global
11 water cycle and vegetation activities. Overall, the global inter-annual series of net primary production
12 (NPP) slightly increased in 2000-2014 at a rate of 0.06 PgC/yr². More than 64% of vegetated land in the
13 Northern Hemisphere showed increased net primary production, while 60.3% of vegetated land in the
14 Southern Hemisphere showed decreased trend. Net primary production correlates positively with land
15 actual evapotranspiration (ET), especially in the Northern Hemisphere, where the increased vegetation
16 productivity (0.13 PgC/yr²) promotes decadal rises of terrestrial evapotranspiration (0.61 mm/yr²).
17 However, anomalous dry conditions led to reduced vegetation productivity (-0.18 PgC/yr²) and nearly
18 ceased growth in terrestrial evapotranspiration in the Southern Hemisphere (0.41 mm/yr²). Under the
19 content of past warmest 15 years, global potential evapotranspiration (PET) shows an increasing trend



20 of 1.72 mm/yr², while precipitation for the domain shows a variability positive trend of 0.84 mm/yr²,
21 which consistent with expected water cycle intensification. But precipitation trend is lower than
22 evaporative demand, indicating some moisture deficit between available water demand and supply for
23 evapotranspiration, thereby accelerated soil moisture loss. Drought indices and
24 precipitation-minus-evaporation suggested an increased risk of drought in the present century.

25 To understand why climates in the northern and southern hemispheres respond differently to NPP, the
26 results showed that temperature is the dominant control on vegetation growth in the high latitude in the
27 Northern Hemisphere, while net radiation is the main effect factors to NPP in the mid latitude, and in
28 arid and semi-arid biomes also mainly driven by precipitation. While in the Southern Hemisphere, NPP
29 decreased because of warming associated drying trends of PDSI.



30 **1 Introduction**

31 Organizations such as the Intergovernmental Panel on Climate Change (IPCC) and the World
32 Meteorological Organization (WMO) have reported that the recent decade was the warmest on record.
33 Warming indicating a general prospective acceleration or intensification of the global hydrological cycle
34 and thus alters evapotranspiration (Wentz et al., 2007; Douville et al., 2013), with implications for the
35 response and mutual feedbacks of ecosystem services (Jung et al., 2010; Davie et al., 2013). Most of the
36 research analyzed the impacts of climate change on vegetation activities, and some research on
37 feedback of terrestrial ecosystems to climate change has focused on their potential role as carbon
38 sources (Field et al., 2007). Fewer study revealed the feedback of vegetation interannual variability on
39 the land surface physical processes and climate system (Zhi et al., 2009), especially on
40 evapotranspiration.

41 Terrestrial net primary production (NPP), defines as the amount of photosynthetically fixed carbon
42 available to the first heterotrophic level in an ecosystem, links terrestrial biota with the atmosphere
43 system (Beer et al., 2010). There have been considerable efforts of ecosystem models to estimate
44 terrestrial NPP, owing to its importance for ecological and social systems at continental and global
45 scales (Chen et al., 2012; Potter et al., 2012; Pan et al., 2014). Several studies have shown that climate
46 constraints (e.g. with increasing temperature and solar radiation) were relaxing (Nemani et al., 2003).
47 The interaction of temperature, radiation and water has imposed complex and varying limitations on
48 vegetation activities in different regions of the world. The spatial variation of NPP depends on regional
49 soil and climatic conditions, vegetation types, and human activities, while the temporal variation of NPP



50 depends on the annual and seasonal variability of climatic factors. The temporal-spatial variation and
51 attribution in global terrestrial NPP under the content of high variability warming are still lacking.

52 In turn, vegetation productivity influences albedo and emissivity, which strongly regulates global
53 climate (Chapin et al., 2011), which is especially obvious in land evapotranspiration. Land
54 evapotranspiration is a central process in the climate system and a nexus of the water, energy and
55 carbon cycles. Hence, it plays a pivotal role in maintaining the water and heat balance. Shen and
56 colleagues (2015) reported that, in contrast with the Arctic region (i.e., positive feedback to warming),
57 increased vegetation activity may attenuate daytime warming by enhancing actual evapotranspiration as
58 a cooling process on the Tibetan Plateau. Zhang et al. (2015) investigated that climate change and recent
59 vegetation greening promote multi-decadal rises of global land evapotranspiration, while anomalous
60 drought between 2000 and 2009 led to reduced vegetation productivity in the Southern Hemisphere
61 (Zhao and Running, 2010). However, little observational evidence exists to demonstrate vegetation
62 feedback on climate in different global geographical units.

63 Investigating factors that control changes in NPP and its feedback effects could provide important
64 clues to the underlying mechanisms and the complex interactions between ecosystems and climate
65 systems (Tian et al., 2000; 2012). Having a clear understanding of the land's biophysical feedback to the
66 atmosphere is crucial if we are to simulate regional climate accurately. In our study, we investigated: 1)
67 whether the high volatility temperature of the past decade continued to increase NPP, or if different
68 climate constraints were at play. 2) why climates in the northern and southern hemispheres respond
69 differently to NPP? 3) what is the temporal-spatial variation of NPP and its feedback to
70 evapotranspiration?



71 **2 Data and Methodology**

72 **2.1 Data**

73 The monthly grid data of the temperature and precipitation series (2000-2014), with the spatial
74 resolution of 0.5 degree, were collected from the Climatic Research Unit
75 (<http://www.cru.uea.ac.uk/data/>).

76 The radiation and soil moisture data series were come from Global Land Data Assimilation System
77 (GLDAS-1), with the spatial resolution of 0.25 degree ([http://gdata1.sci.gsfc.nasa.gov/daac-bin/](http://gdata1.sci.gsfc.nasa.gov/daac-bin/G3/gui.cgi?instance_id=GLDAS025_M)
78 [G3/gui.cgi?instance_id=GLDAS025_M](http://gdata1.sci.gsfc.nasa.gov/daac-bin/G3/gui.cgi?instance_id=GLDAS025_M)). The depths of the four soil layers are: 0-10 cm, 10-40 cm,
79 40-100 cm, and 100-200 cm. The quality of the GLDAS data set was assessed against available
80 observations from multiple sources (Zhang et al., 2008; Chen et al., 2013).

81 The monthly data of Palmer Drought Severity Index (PDSI), with the spatial resolution of 2.5 degree,
82 was available at <http://www.cgd.ucar.edu/cas/catalog/ climind/pdsi.html>. PDSI, as a indicator of land
83 surface moisture conditions, has been widely used in routinely monitoring and assessing global and
84 regional drought conditions. The global dry areas were defined as $PDSI < -3.0$, while the wet areas were
85 defined as $PDSI > + 3.0$ (Dai et al., 2004).

86 We used the Global Land Cover Characterization data from the International Geosphere-Biosphere
87 Program (IGBP) in 2000 (<http://edc2.usgs.gov/glcc/glcc.php>), and MODIS in 2000 and 2013
88 (<http://modis.gsfc.nasa.gov/data/dataproduct/mod12.php>). From these data, a routinely integrated
89 classification of land use/cover change (LUCC) characteristics can be obtained based on the feature
90 fusion processes.



91 We unified the spatio-temporal resolution of these data from different sources based on the
92 re-sampling and re-classification techniques.

93 2.2 Methods

94 *NPP algorithm.* Net primary production estimations are typically model-based and biogeochemical,
95 generated from a larger set of simulated C fluxes between the atmosphere and terrestrial ecosystems (Ito
96 et al., 2011). The global 1-km MODIS NPP datasets from 2000 to 2014 are from MOD17. A better
97 agreement of MODIS and terrestrial NPP estimates allows for the use of MODIS in large-scale
98 estimates (Neumann et al., 2015). The algorithm calculates annual NPP as:

$$99 \quad NPP = \sum_{i=1}^{365} (GPP - R_m) - R_g \quad (1)$$

100 Similarly, the algorithm calculates daily GPP as:

$$101 \quad GPP = \varepsilon_{\max} \times SW_{rad} \times FPAR \times fVPD \times fT_{\min} \quad (2)$$

102 R_m is the maintenance respiration, which is a function of daily average temperature (T_{avg}):

$$103 \quad R_m = Q_{10}^{\left(\frac{T_{avg}-20}{10}\right)} \quad (3)$$

$$104 \quad Q_{10} = 3.22 - 0.046 \times T_{avg} \quad (4)$$

105 Therefore,

$$106 \quad NPP = \sum_{i=1}^{365} (GPP - R_m) - R_g = \sum_{i=1}^{365} (GPP - R_m) - 0.25 \times NPP \quad (5)$$

107 which means:



108
$$NPP = 0.8 \times \sum_{i=1}^{365} (GPP - R_m), \quad \text{where } \sum_{i=1}^{365} (GPP - R_m) \geq 0 \quad (6)$$

109
$$NPP = 0, \quad \text{where } \sum_{i=1}^{365} (GPP - R_m) < 0 \quad (7)$$

110 where ϵ_{\max} is the maximum light use efficiency, SW_{rad} is short-wave downward solar radiation (of
111 which 45% is Photosynthetically Active Radiation (PAR)), FPAR is the fraction of PAR being absorbed
112 by the plants, fVPD and fT_{\min} are the reduction scalar from high daily time Vapor Pressure Deficit and
113 low daily minimum temperature (T_{\min}), respectively, and annual growth respiration (R_g) is a function of
114 annual maximum leaf area index (LAI). Zhao and Running (2010) modified the calculations by
115 assuming that growth respiration is approximately 25% of NPP.

116 *ET and PET algorithm.* The MODIS evapotranspiration datasets are estimated using Mu and
117 colleagues (2011) improved ET algorithm over Mu et al.'s (2007) previous paper. Based on the
118 energy-balance theory and the Penman-Monteith equation, the required MODIS data inputs ET
119 algorithms, including daily meteorology (temperature, actual vapor pressure, and incoming solar
120 radiation) remotely-sensed land cover, FPAR/LAI, and albedo (Friedl et al., 2002, 2010; Myneni et al.,
121 2002; Jin et al., 2003). The output variables include evapotranspiration (ET), latent heat flux (LE),
122 potential ET (PET), potential LE (PLE) and quality control (ET_QC).

123 *Trend analysis.* To further discern the trends of yearly NPP and ET, we examined linear trends
124 estimation on a per-pixel basis to establish a linear regression relationship between variables (x_i) and
125 time (t_i). The regression coefficient (b) is:



126

$$b = \frac{n \times \sum_{i=1}^n x_i t_i - \sum_{i=1}^n x_i \sum_{i=1}^n t_i}{n \times \sum_{i=1}^n t_i^2 - \left(\sum_{i=1}^n t_i \right)^2} \quad (8)$$

127

128

129

Partial correlation analysis. This method is used to describe the relationship between two variables while taking away the effects of several other variables. The partial correlation of x_1 and x_2 is adjusted for a third variable y (at a significance level of 0.05 by t-text):

130

$$r_{x_1 x_2 \cdot y} = \frac{r_{x_1 x_2} - r_{x_1 y} r_{x_2 y}}{\sqrt{(1 - r_{x_1 y}^2)(1 - r_{x_2 y}^2)}} \quad (9)$$

131

3 Results and analysis

132

3.1 Temporal-spatial variation in global terrestrial NPP and its feedback to ET

133

134

135

136

137

138

139

140

141

The spatial pattern of global NPP trend (2000-2014) steadily decreasing from the equator to the Arctic and Antarctic (Fig. 1c). Overall, the inter-annual series of NPP increased moderately at a rate of 0.06 PgC/yr² throughout the last 15 years. Additionally, it shows different changes in the Northern Hemisphere (NH) and Southern Hemisphere (SH). While increasing over large areas in the NH (Fig. 1a), decreased in the SH (Fig. 1b). Specifically, in the NH, 64% of vegetated area had increased NPP, including large areas of North America, Western Europe, India, and the eastern China. Regions with decreased NPP include east Europe, high latitudes of central and west Asia. In the SH, decreased NPP accounted for about 60.3% of vegetated land area, mainly concentrated in the large parts of South America, south Africa, and west Australia. Furthermore, in the equatorial regions, Amazon rainforests



142 had significantly decreased NPP, whereas African rainforests experienced an increasing trend (Fig. 1c).
143 Because tropical rainforest NPP accounts for a large proportion of global NPP, decreases in the SH
144 partially counteracted increases in NH.

145 By combining the global land use/cover change (LUCC) characteristics, the results showed that
146 shrubland has the greatest potential increasing trend of NPP (16.5 gC/m²/yr) compared to other biomes,
147 followed by grassland (12.5 gC/m²/yr). This may be related to the expansion of woody vegetation over
148 the past 15 years. In Arctic tundra (Hughes et al., 2006) and lower latitudes in arid environments (Chen
149 et al., 2014), experimental studies provided clear evidence that climate warming is sufficient to account
150 for the expansion of shrubs and graminoids.

151 Changes in vegetation albedo and emissivity exert feedback on climate, which is especially obvious
152 in evapotranspiration (Field et al., 2007). Increased vegetation productivity and climate change promote
153 multi-decadal rises of global land ET (Zhang et al., 2015). The average mean of estimated global annual
154 ET is 518.6 mm/yr, with an inter-annual trend of 0.46 mm/yr². Figure 1a&1b showed that NPP
155 correlates positively with ET (especially in the NH, however, reduced vegetation productivity nearly
156 ceased growth in ET in SH). The variations anomaly in the SH has a much higher variability, so the
157 consistency between NPP and ET in the SH is less than that in the NH. The spatial inconsistency in the
158 SH mainly occurred near the equator, e.g., southern African rainforests (Fig. 1b&1d). These regions
159 have high values of average annual precipitation and stronger variability than elsewhere, causing greater
160 changes to ET and its components (land surface evaporation, canopy evaporation and transpiration).
161 When the inter-annual variability of NPP is small, the ET component of land surface evaporation
162 increases. In contrast, in areas with large inter-annual variability of NPP such as shrubland and grass



163 dominant regions, the ET components of land surface evaporation declines and transpiration increases.

164 **3.2 Major climatic control factors to NPP variation**

165 To understand why climates in the northern and southern hemispheres respond differently to NPP, we
166 first estimated the spatial trends of climatic control factors, and then analyzed the complex multiple
167 climatic constraints to plant growth. A comprehensive interpretation of interactive climatic controls on
168 plant productivity showed that water, temperature and radiation are the key factors affecting vegetation
169 growth. Globally, growth was most strongly limited by water availability on 40% of Earth's vegetated
170 surface, while temperature limitations exerted the main controlling influence on 33%, and radiation on
171 27% (Nemani et al., 2003).

172 From 2000 to 2014, overall trends of average annual temperature ($0.007\text{ }^{\circ}\text{C}/\text{yr}^2$) and precipitation
173 ($0.84\text{ mm}/\text{yr}^2$) experienced world-wide increases while showing different temporal change patterns (Fig.
174 2a & 2b). Eastern Europe, South America, southern Africa and western Australia experienced warming
175 combined with decreased precipitation (warm-dry trend), whereas southeast North America, western
176 Europe, east Russia, and African rainforests experienced warming combined with increased
177 precipitation (warm-wet trend). Meanwhile, net radiation (R_n) increased in the equatorial tropics and
178 arid regions in Northwestern China, but decreased in the Arctic and Antarctic (Fig. 2c). The Palmer
179 Drought Severity Index (PDSI) is a widely-used drought index that correlates with soil moisture during
180 warm seasons (Dai et al., 2004; 2013). Generally, a lower PDSI implies a drier climate. Global PDSI
181 has decreased at a rate of $0.04/\text{yr}^2$ over the past 15 years. This suggests an increased risk of drought in
182 the twenty-first century. The spatial trend of PDSI shows that the eastern and northern coasts of North



183 America, along with the African continent, Eurasia and southern South America, had obvious drought
184 trends from 2000-2014. Northern China, parts of Mongolia, and western Russia near Lake Baikal also
185 experienced a drying trend (Fig. 2d). Warming-induced drying resulted from increased ET, and was
186 most prevalent over NH mid-high latitudes. Drought develops with periods of low accumulated
187 precipitation and is exacerbated by high temperatures.

188 We analyzed partial correlations between NPP and temperature (T), precipitation (P), Net radiation
189 (Rn) and PDSI during growing seasons to determine their respective contributions across different
190 regions (Fig. 3, Table 1). Climate changes from 2000 to 2014 have made temperature, precipitation and
191 radiation somewhat beneficial to plant growth. In the NH, climatic changes have eased multiple climatic
192 constraints to plant growth in an earlier spring, but the continuous warming may offset the benefits.

193 In NH high latitudes ($>47.5^{\circ}\text{N}$), temperature has a positive correlation with NPP ($R=0.6$). Significant
194 warming generally lengthens the vegetation growing seasons and promotes plant growth in tundra
195 regions, so the recent warming in this region has increased NPP (Fig. 3a). For northern mid and low
196 latitudes ($<47.5^{\circ}\text{N}$), where large areas are classified as having an arid climate, vegetation is short-rooted.
197 NPP has a significant negative correlation with P ($R=0.7$, $p<0.05$) (Fig. 3b) and is also correlated to Rn
198 (Fig. 3c). In areas of high elevation such as the Tibetan plateau (which is similar to high latitudes),
199 temperature is the dominant control factor in vegetation growth.

200 Equatorial Amazon rainforests experienced significantly decreased NPP, whereas African rainforests
201 exhibited an increasing trend. These changes in equatorial regions are mainly related to the warming in
202 the Amazon along with increasing precipitation in African rainforests. High temperatures cause higher
203 rates of evapotranspiration, generally reducing soil water availability for vegetation in Amazon.



204 For the SH, we noted a significant correlation ($r = 0.7$, $p < 0.05$) between NPP and PDSI (Fig. 3d). The
205 warming trend induced a much higher evaporative demand and led to a drying trend, except for the
206 afore-mentioned increased precipitation in African rainforests. The PDSI in African rainforests also
207 showed a slight increasing trend. The general drought event across the SH, which was induced by
208 extreme heat and precipitation deficit, has resulted in a net water availability reduction. Warming
209 associated drying directly caused the significantly decreasing trend of NPP in SH.

210 **3.3 Continuation feedback of NPP to evapotranspiration likely exacerbate regional drought**

211 Drought indices suggested an increased risk of drought in the present century. We used potential
212 evapotranspiration (PET) as a surrogate measure of atmospheric moisture demand. Potential
213 evapotranspiration is defined as the maximum quantity of water capable of being evaporated from the
214 soil and transpired from the vegetation, and actual evapotranspiration is the actual evaporation from
215 water and soil, and transpiration from vegetation. Penman (1948) stated that ET had a proportional
216 relationship with PET, and Bouchet (1963) hypothesized that a complementary feedback mechanism
217 exists between ET and PET in water-limited regions. Overall, our investigations do indicate that there is
218 a proportional behavior between ET and PET in humid regions and a complementary one in arid regions
219 (Fig. 1d and Fig. 4a). PET, combined impacts of temperature, solar radiation, vapor pressure and wind
220 speed (Zhang et al., 2015), has an interaction process with NPP (Fig. 4b).

221 Global PET shows an increasing trend of 1.72 mm/yr^2 over the past 15-year record, while P for the
222 domain shows a variability positive trend of 0.84 mm/yr^2 . It indicates some moisture deficit between
223 available water demand and supply for evapotranspiration. P is mostly being lost to ET rather than being



224 allocated to other components of energy and water cycle (Zhang et al., 2015).

225 Soil moisture is an important sensor for measuring surficial wetness and dryness levels, which almost
226 reflects the dryness and wetness of climate. With precipitation being the most direct factor influencing
227 on soil moisture, temperature and solar radiation etc. mainly through evapotranspiration to cause soil
228 moisture loss. Available soil moisture is defined as the amount of water a plant can access in its root
229 zone. Thus, spatial and temporal variations in soil moisture closely related to vegetation growth (Davis
230 and Pelsor, 2001; Yang et al., 2010). Figure 5 illustrates the world-wide decrease in soil moisture in four
231 layers (0-10, 10-40, 40-100, and 100-200 cm). The increasing soil moisture limitation is a classic
232 eco-hydrologically-confined factor.

233 **4 Discussions**

234 Earth experienced dramatic environmental changes in the recent 15 years of the 21st century.
235 Although a relatively short time series analysis (2000-2014), a strong variation of NPP and its feedback
236 to evapotranspiration, as well as the correlation with the dramatic climate changes were found
237 worldwide. There are some uncertainties in the feedbacks of ecosystem responses to evapotranspiration,
238 but understanding the land-surface ecological feedbacks to the atmosphere processes is necessary if we
239 are willing to simulate climate change accurately. Several studies showed that the relaxed climate
240 constraints with increasing temperature and solar radiation, allowed an increased trend in global NPP
241 over 1982-1999 (Nemani et al., 2003). This was followed by a drought-induced reduction in global NPP
242 in 2000-2009 (Zhao and Running, 2010). Our study used global 1-km MODIS NPP datasets from 2000
243 to 2014. The results showed that under the content of past warmest 15 years, the slightly increased



244 inter-annual series of NPP promote decadal rises of global land ET, thereby accelerated soil moisture
245 loss. Weather systems can lead to droughts by suppressing precipitation (Beaumont et al., 2011) and by
246 warming and drying soil via soil-temperature feedback (Seneviratne et al., 2010; Sheffield et al., 2012;
247 Orłowsky and Seneviratne, 2013; Williams et al., 2014). Drought indices and precipitation-minus
248 -evaporation suggested an increased risk of drought in the present century.

249 As noted previously, vegetation feeds back to the spatio-temporal characteristics of climate through
250 evapotranspiration. Evapotranspiration is a key process that dissipates the energy and water absorbed by
251 the vegetation and determines the diurnal cycle of near-surface temperature. It is limited mostly by
252 energy in humid and semi-humid areas, whereas low-value evapotranspiration is limited mostly by
253 water in arid and semi-arid areas. The different values of average precipitation and variability as well as
254 different land types will cause diverse changes in evapotranspiration and its components (land surface
255 evaporation, canopy evaporation and transpiration), thereby producing different feedback to temperature.
256 There are still major gaps in our understanding of how the responses of terrestrial ecosystems eliminate
257 or increase the risk of dangerous climate change, and these gaps need to be filled.

258 **5 Conclusions**

259 The inter-annual series of global NPP slightly increased for the last 15 years but has different changes
260 in the Northern Hemisphere and Southern Hemisphere. Over 64% of vegetated land areas had increased
261 NPP in the Northern Hemisphere while 60.3% had decreased NPP in the Southern Hemisphere. In the
262 Northern Hemisphere, temperature is the dominant control on vegetation growth in the high latitude,
263 while net radiation is the main effect factors to NPP in the mid latitude, and in arid and semi-arid



264 biomes also mainly driven by precipitation. In the Southern Hemisphere, NPP decreased because of
265 warming associated drying trends of PDSI.

266 NPP to actual evapotranspiration are likely to be positive feedback, especially significant in the
267 Northern Hemisphere, where the increased vegetation productivity (0.13 PgC/yr^2) reduces albedo,
268 promotes decadal rises of actual evapotranspiration (0.61 mm/yr^2). However, dry conditions led to
269 reduced vegetation productivity (-0.18 PgC/yr^2) and nearly ceased growth in evapotranspiration in the
270 Southern Hemisphere. Continuation of these trends will likely exacerbate regional drought levels.

271 **Author Contribution**

272 Zhi Li and Yaning Chen wrote the main manuscript text, YangWang and Gonghuan Fang prepared
273 figures 4&6. All authors reviewed the manuscript.

274 **Acknowledgements**

275 The research is supported by the CAS "Light of West China" Program (2015XBQNB17) and the
276 Foundation of State Key Laboratory of Desert and Oasis Ecology (Y471166).

277 **References**

- 278 Beaumont, L.J., Pitman, A., Perkins, S., Zimmermann, N.E., Yoccoz, N.G., and Thuiller, W.: Impacts of climate
279 change on the world's most exceptional ecoregions, P. Natl. Acad. Sci. USA., 108(6), 2306-2311, doi:
280 10.1073/pnas.1007217108, 2011.
- 281 Beer, C., Reichstein, M., Tomelleri, E., Ciais, P., Jung, M., Carvalhais, N., Rödenbeck, C., Arain, M.A., Baldocchi, D.,



- 282 Bonan, G.B., Bondeau, A., Cescatti, A., Lasslop, G., Lindroth, A., Lomas, M., Luysaert, S., Margolis, H., Oleson,
283 K.W., Rouspard, O., Veenendaal, E., Viovy, N., Williams, C., Woodward, F.I., and Papale, D.: Terrestrial gross
284 carbon dioxide uptake: global distribution and covariation with climate, *Science*, 329(5993), 834-838, doi:
285 10.1126/science.1184984, 2010.
- 286 Bouchet, R.J.: Evapotranspiration reele et potentielle, signification climatique, General Assembly of Berkeley, Red
287 Book, 62, 134-142, IAHS, Gentbrugge, Belgium, 1963.
- 288 Chapin, F.S., Matson, P.A., and Vitousek P.M.: Principles of terrestrial ecosystem ecology, Springer, New York, 2011.
- 289 Chen, G.S., Tian, H.Q., Zhang, C., Liu, M.L., Ren, W., Zhu, W.Q., Chappelka, A.H., Prior, S.A. and Lockaby, G.B.:
290 Drought in the Southern United States over the 20th century: Variability and its impacts on terrestrial ecosystem
291 productivity and carbon storage, *Climatic Change*, 114(2), 379-397, doi: 10.1007/s10584-012-0410, 2012.
- 292 Chen, L.Y., Li, H., Zhang, P.J., Zhao, X., Zhou, L.H., Liu, T.Y., Hu, H.F., Bai, Y.F., Shen, H.H., and Fang J.Y.: Climate
293 and native grassland vegetation as drivers of the community structures of shrub-encroached grasslands in Inner
294 Mongolia, China, *Landscape Ecol.*, doi: 10.1007/s10980 -014-0044-9, 2014.
- 295 Chen, Y. K., Yang, J., Qin, L., Tang, W.Z., and Han, M.: Evaluation of AMSR - E retrievals and GLDAS simulations
296 against observations of a soil moisture network on the central Tibetan Plateau, *J. Geophys. Res.*, 118(10), 4466-4475,
297 doi: 10.1002/jgrd.50301, 2013.
- 298 Dai, A.G., Trenberth, K.E., and Qian, T.T.: A global dataset of Palmer Drought Severity Index for 1870-2002:
299 relationship with soil moisture and effects of surface warming, *J. Hydrometeorol.*, 5, 1117-1130, doi:
300 10.1175/JHM-386.1, 2004.
- 301 Dai, A.: Increasing drought under global warming in observations and models. *Nat. Clim. Change*, 3, 52-58, doi:
302 10.1038/nclimate1633, 2013.
- 303 Davie, J.C.S., Falloon, P.D., Kahana, R., Dankers, R., Betts, R., Portmann, F.T., Wisser, D., Clark, D.B., Ito, A.,
304 Masaki, Y., Nishina, K., Fekete, B., Tessler, Z., Wada, Y., Liu, X., Tang, Q., Hagemann, S., Stacke, T., Pavlick, R.,
305 Schaphoff, S., Gosling, S.N., Franssen, W., and Arnell, N.: Comparing projections of future changes in runoff from



- 306 hydrological and biome models in ISI-MIP, *Earth Syst. Dynam.*, 4, 359-374, doi:10.5194/esd-4-359-2013, 2013.
- 307 Davis, M.A., and Pelsor M.: Experimental support for a resource-based mechanistic model of invisibility, *Ecol. Lett.*, 4,
- 308 421-428, doi: 10.1046/j.1461-0248.2001.00246.x, 2001.
- 309 Douville, H., Ribes, A., Decharme, B., Alkama, R. and Sheffield, J.: Anthropogenic influence on multidecadal changes
- 310 in reconstructed global evapotranspiration, *Nat. Clim. Change*, 3, 59-62, doi: 10.1038/NCLIMATE1632, 2013.
- 311 Field, C.B., Lobell, D.B., Peters, H.A. and Chiariello, N.R.: Feedbacks of terrestrial ecosystems to climate change,
- 312 *Annu. Rev. Environ. Resour.*, 32, 1-29, doi: 10.1146/annurev.energy.32.053006.141119, 2007.
- 313 Friedl, M.A., McIver, D.K., Hodges, J.C.F., Zhang, X.Y., Muchoney, D., Strahler, A.H., Woodcock, C.E., Gopal, S.,
- 314 Schneider, A., Cooper, A., Baccini, A., Gao, F., and Schaaf, C.: Global land cover mapping from MODIS:
- 315 Algorithms and early results, *Remote Sens. Environ.*, 83(1-2), 287-302, doi: 10.1016/S0034-4257(02)00078-0,
- 316 2002.
- 317 Friedl, M.A., Sulla-Menashe, D., Tan, B., Schneider, A., Ramankutty, N., Sibley, A., Huang, X.M.: MODIS Collection
- 318 5 global land cover: Algorithm refinements and characterization of new datasets, *Remote Sens. Environ.*, 114(1),
- 319 168-182, doi: 10.1016/j.rse.2009.08.016, 2010.
- 320 Hughes, R.F., Archer, S.R., Asner, G.P., Wessman, C.A., McMurtry, C., Nelson, J., Ansley, R.J.: Changes in
- 321 aboveground primary production and carbon and nitrogen pools accompanying woody plant encroachment in a
- 322 temperate savanna, *Glob. Change Biol.*, 12, 1733-1747, doi: 10.1111/j.1365-2486.2006.01210.x, 2006.
- 323 Ito, A.: A historical meta-analysis of global terrestrial net primary productivity: Are estimates converging, *Global*
- 324 *Change Biol.*, 17, 3161-3175, doi: 10.1111/j.1365-2486.2011.02450.x, 2011.
- 325 Jin, Y., Schaaf, C.B., Woodcock, C.E., Gao, F., Li, X., Strahler, A.H., Lucht, W., and Liang, S.L.: Consistency of
- 326 MODIS surface BRDF/Albedo retrievals: 2. Validation, *J. Geophys. Res.*, 108(D5), 4159, doi:
- 327 10.1029/2002JD002804, 2003.
- 328 Jung, M., Reichstein, M., Ciais, P., Seneviratne, S.I., Sheffield, J., Goulden, M.L., Bonan, G., Cescatti, A., Chen, J.Q.,
- 329 Jeu, de R., Dolman, A.J., Eugster, W., Gerten, D., Gianelle, D., Gobron, N., Heinke, J., Kimball, J., Law, B.E.,



- 330 Montagnani, L., Mu, Q.Z., Mueller, B., Oleson, K., Papale, D., Richardson, A.D., Roupsard, O., Running, S.,
331 Tomelleri, E., Viovy, N., Weber, U., Williams, G., Wood, E., Zaehle, S., and Zhang, K.: Recent decline in the
332 global land evapotranspiration trend due to limited moisture supply, *Nature*, 467, 951-954, doi:10.1038/nature09396,
333 2010.
- 334 Mu, Q., Heinsch, F.A., Zhao, M., and Running, S.W.: Development of a global evapotranspiration algorithm based on
335 MODIS and global meteorology data, *Remote Sens. Environ.*, 111, 519-536, doi: 10.1016/j.rse.2007.04.015, 2007.
- 336 Mu, Q., Zhao, M., and Running, S.W.: Improvements to a MODIS global terrestrial evapotranspiration algorithm.
337 *Remote Sens. Environ.*, 115(8), 1781-1800, doi:10.1016/j.rse.2011.02.019, 2011.
- 338 Myneni, R.B., Hoffman, S., Knyazikhin, Y., Privette, J.L., Glassy, J., Tian, Y., Wang, Y., Song, X., Zhang, Y., Smith,
339 G.R., Lotsch, A., Friedl, M., Morisette, J.T., Votava, P., Nemani, R.R., and Running, S.W.: Global products of
340 vegetation leaf area and fraction absorbed PAR from year one of MODIS data, *Remote Sens. Environ.*, 83(1-2),
341 214-231, 2002.
- 342 Nemani, R.R., Keeling, C.D., Hashimoto, H., Jolly, W.M., Piper, S.C., Tucker, C.J., Myneni, R.B., Running, S.W.:
343 Climate-driven increases in global terrestrial net primary production from 1982 to 1999, *Science*, 300, 1560-1563,
344 doi: 10.1126/science.1082750, 2003.
- 345 Neumann, M., Zhao, M.S., Kindermann, G., and Hasenauer, H.: Comparing MODIS net primary production estimates
346 with terrestrial national forest inventory data in Austria, *Remote Sens.*, 7, 3878-3906, doi:10.3390/rs70403878,
347 2015.
- 348 Orlowsky, B., and Seneviratne, S.I.: Elusive drought: uncertainty in observed trends and short- and long-term CMIP5
349 projections, *Hydrol. Earth Syst. Sci.*, 17, 1765-1781, doi: 10.5194/hess-17-1765-2013, 2013.
- 350 Pan, S.F., Tian, H.Q., Dangal, S.R., Zhang, C., Yang, J., Tao, B., Ouyang, Z.Y., Wang, X.K., Lu, C.Q., Ren, W., Banger,
351 K., Yang, Q.C., Zhang, B.W. and Li, X.: Complex spatiotemporal responses of global terrestrial primary production
352 to climate change and increasing atmospheric CO₂ in the 21st century. *PloS One*, 9, e112810, doi:
353 10.1371/journal.pone.0112810, 2014.



- 354 Penman, H.L.: Natural evaporation from open water, bare and grass, P. Roy. Soc. London, 193, 120-145, 1948.
- 355 Potter, C.S., Klooster, S. and Genovese, V.: Net primary production of terrestrial ecosystems from 2000 to 2009,
356 Climatic Change, 115(2), 365-378, doi: 10.1007/s10584-012-0460-2, 2012.
- 357 Seneviratne, S.I., Corti, T., Davin, E.L., Hirschi, M., Jaeger, E.B., Lehner, I., Orlowsky, B., and Teuling, A.J.:
358 Investigating soil moisture–climate interactions in a changing climate: A review, Earth-Sci. Rev., 99(3-4), 125-161,
359 doi: 10.1016/j.earscirev.2010.02.004, 2010.
- 360 Sheffield, J., Wood, E.F., and Roderick, M.L.: Little change in global drought over the past 60 years, Nature, 491,
361 435-438, doi: 10.1038/nature11575, 2012.
- 362 Shen, M.G., Piao, S.L., Jeong, S.J., Zhou, L.M., Zeng, Z.Z., Ciais, P., Chen, D.L., Huang, M.T., Jin, C.S., Li, L.Z.X.,
363 Li, Y., Myneni, R.B., Yang K., Zhang, G., Zhang, Y.J., and Yao, T.D.: Evaporative cooling over the Tibetan Plateau
364 induced by vegetation growth, P. Natl. Acad. Sci. USA., 112(30), 9299-9304, doi: 10.1073/pnas.1504418112, 2015.
- 365 Tian, H., Melillo, J., Kicklighter, D., McGuire, A.D., Iii, J.H., Iii, B.M., and Vörösmarty, C.J.: Climatic and biotic
366 controls on annual carbon storage in Amazonian ecosystems, Global Ecol. Biogeogr., 9(4), 315-335, doi: 10.
367 1046/j.1365-2699.2000.00198.x, 2000.
- 368 Wentz, F. J., Ricciardulli, L., Hilburn, K. and Mears, C.: How much more rain will global warming bring? Science, 317,
369 233-235, doi: 10.1126/science.1140746, 2007.
- 370 Williams, I.N., Torn, M.S., Riley, W.J., and Wehner, M.F.: Impacts of climate extremes on gross primary production
371 under global warming, Environ. Res. Lett., 9, 094011, doi:10.1088/1748-9326/9/9/094011, 2014.
- 372 Yang, Y.H., Fang, J.Y., Ma, W.H., Smith, P., Mohammat, A., Wang, S.P. and Wang, W.: Soil carbon stock and its
373 changes in northern China's grasslands from 1980s to 2000s, Glob. Change Biol., 16, 3036-3047, doi:
374 10.1111/j.1365-2486.2009.02123.x, 2010.
- 375 Zhang, J., Wang, W.C. and Wei, J.: Assessing land-atmosphere coupling using soil moisture from the Global Land Data
376 Assimilation System and observational precipitation, J. Geophys. Res., 113(D17), D17119, doi: 10.1029/2008
377 JD009807, 2008.



- 378 Zhang, K., Kimball, J.S., Nemani, R.R., Running, S.W., Hong, Y., Gourley, J.J. and Yu, Z.B.: Vegetation greening and
379 climate change promote multidecadal rises of global land evapotranspiration, *Sci. Rep.*, 5, 15956, doi:
380 10.1038/srep15956, 2015.
- 381 Zhao, M.S., and Running, S.W.: Drought-induced reduction in global terrestrial net primary production from 2000
382 through 2009, *Science*, 329, 940-943, doi: 10.1126/science.1192666, 2010.
- 383 Zhi, H., Wang, P.X., Dan, L., Yu, Y.Q., Xu, Y.F. and Zheng, W.P.: Climate-vegetation interannual variability in a
384 coupled atmosphere-ocean-land model. *Adv. Atmos. Sci.*, 26(3), 599-612, doi: 10.1007/s00376-009-0599-6.



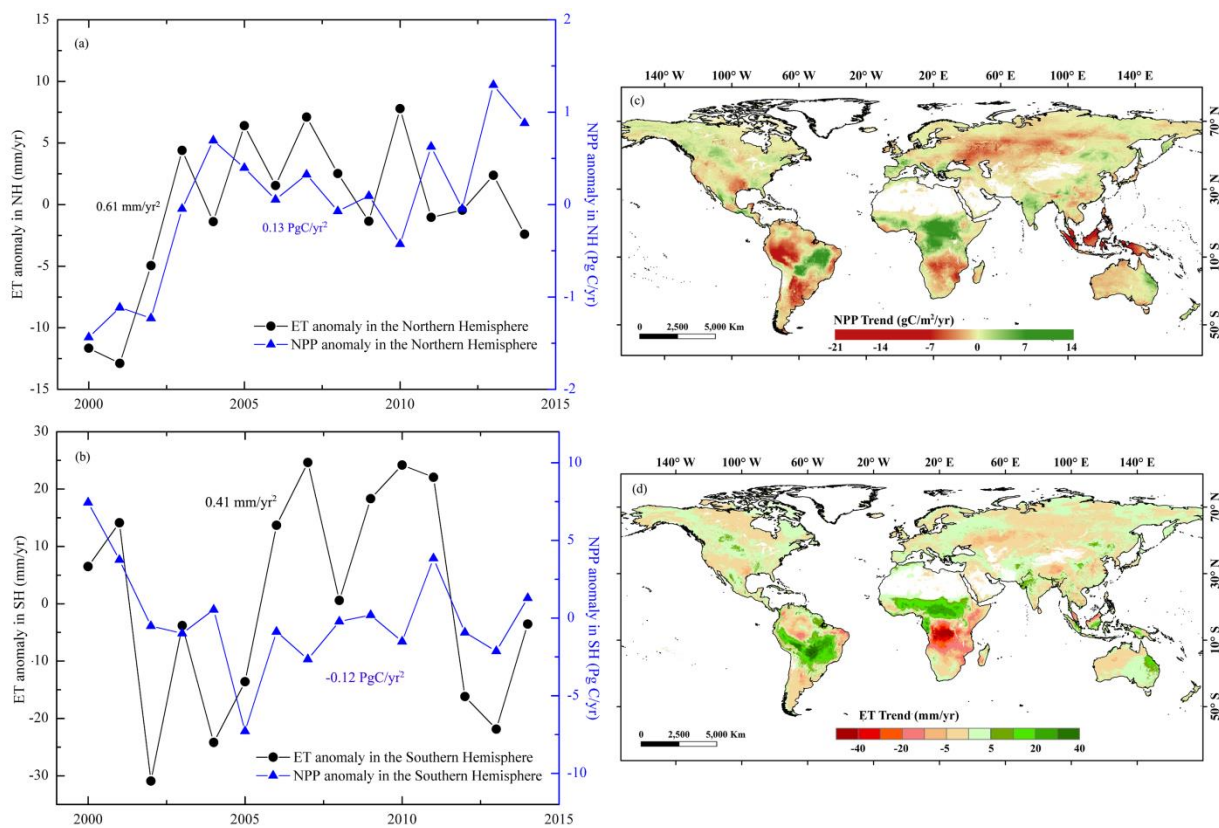
385 **Table:**

386 Table 1. Correlations between NPP and climatic variables for over both hemispheres

Zones	NPP trend	T trend	P trend	Rn trend	PDSI trend
NH high latitudes (>47.5 °N)	$y=0.02x+30.51$	$y=0.021x-5.75$ R= 0.60*	$y=0.104x+46.58$ R=0.29	$y=-5.21x+453.6$ R=0.45	$y=-0.005x+0.23$ R=0.44
NH mid/low latitudes (<47.5 °N)	$y=0.07x+45.68$	$y=0.009x+18.3$ R= -0.17	$y=0.341x+76.8$ R= 0.70**	$y=3.239x+105.9$ R=0.50	$y=0.006x-0.46$ R=0.56
South Hemisphere	$y=-0.18x+78.37$	$y=0.010x+21.6$ R= -0.53	$y=0.074x+116.8$ R=0.37	$y=2.455x+129.4$ R=0.43	$y=-0.042x+0.33$ R= 0.70**

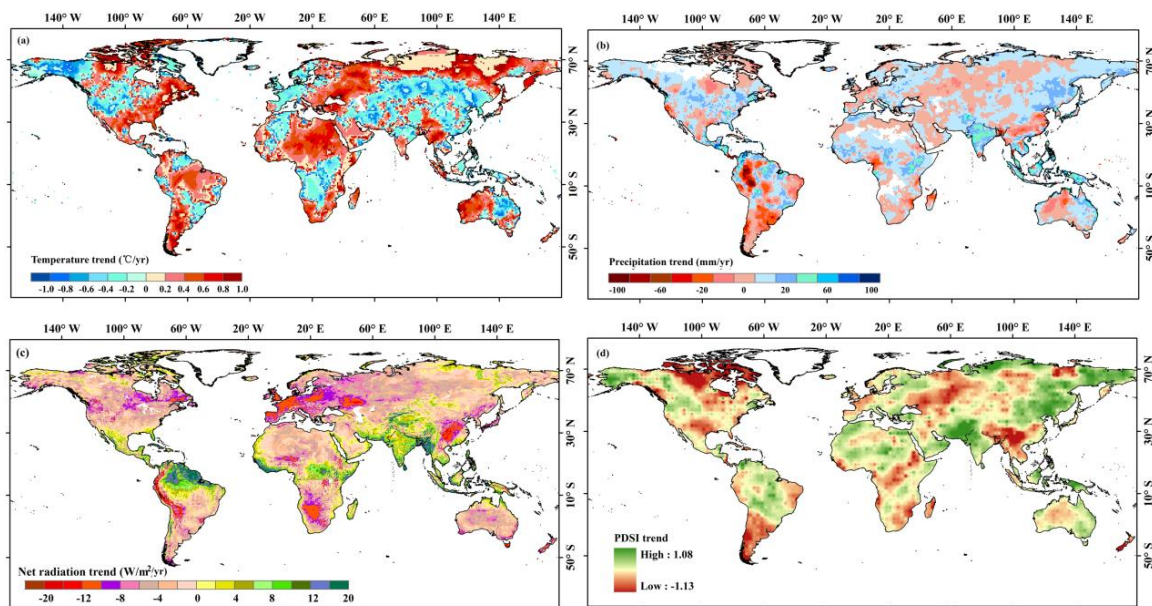
387

388



389

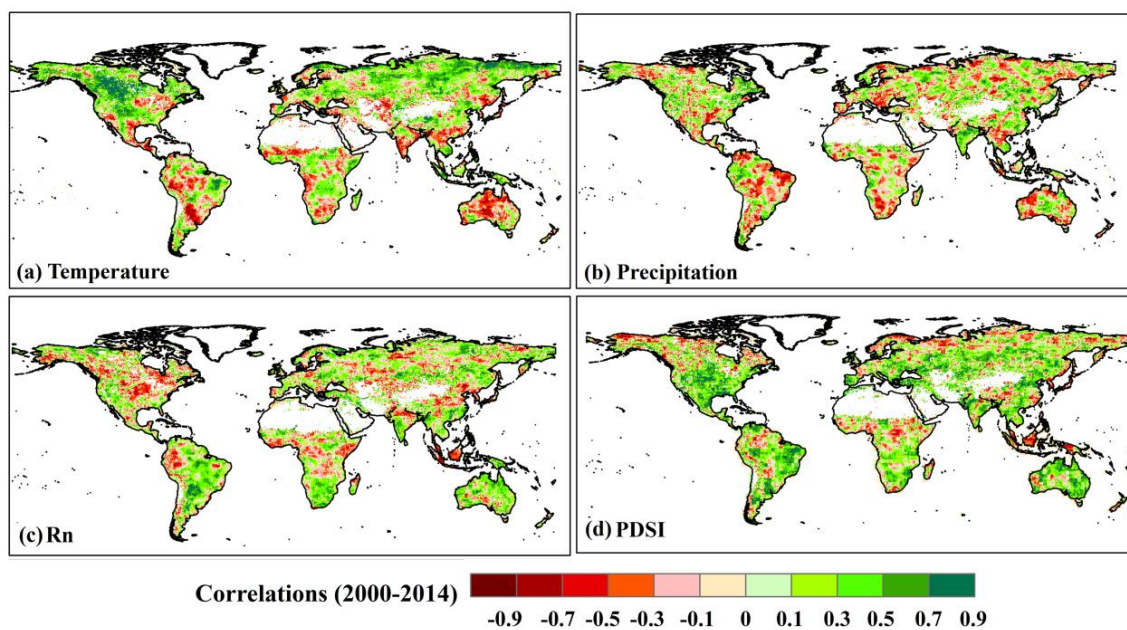
390 Fig. 1. Temporal-spatial variations in global terrestrial NPP and ET from 2000-2014. (a) Inter-annual
 391 variations of NPP and ET in the Northern Hemisphere (NH). (b) Inter-annual variations of NPP and ET
 392 in the Southern Hemisphere (SH). (c) Spatial pattern of NPP trend. (d) Spatial pattern of ET trend.



393

394 Fig. 2. Trends of air temperature (T), precipitation (P), net radiation (Rn) and Palmer Drought Severity

395 Index (PDSI) from 2000-2014.



396

397 Fig. 3. Partial correlations between NPP and (a) Temperature, (b) Precipitation, (c) Net radiation, (d)

398 PDSI in growing season.

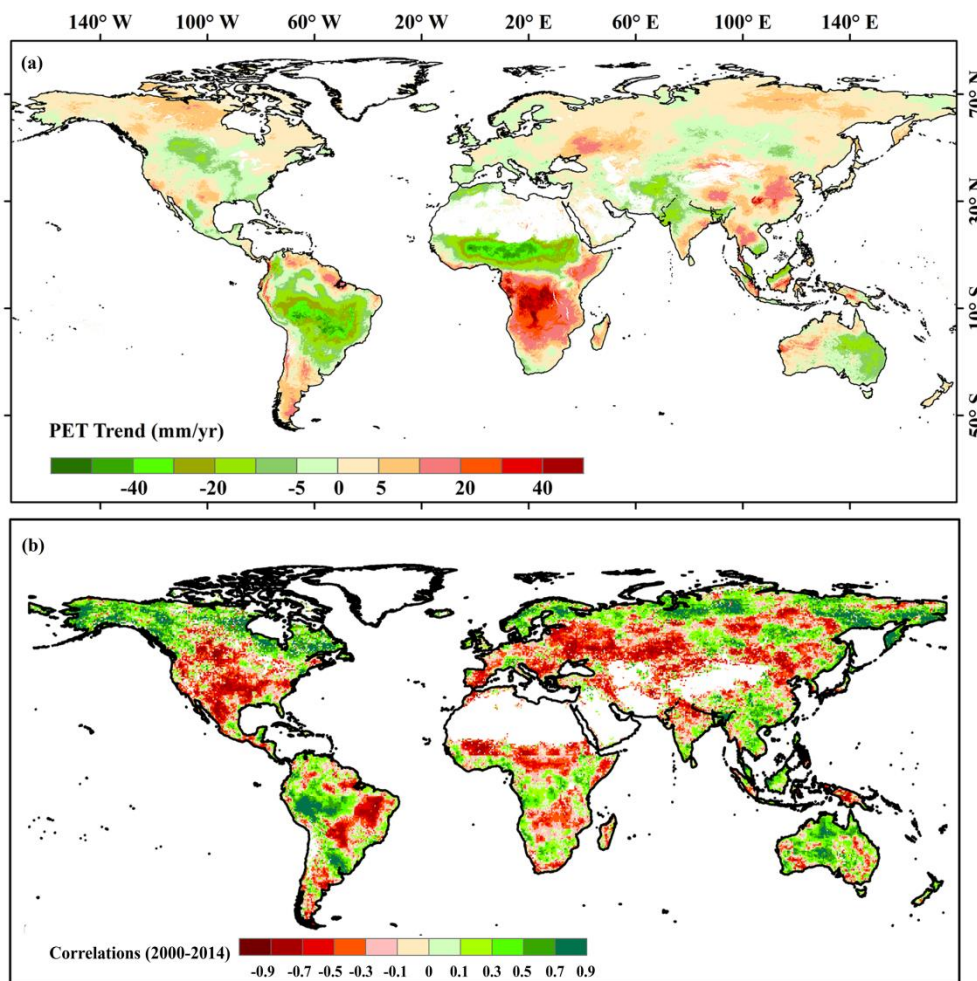
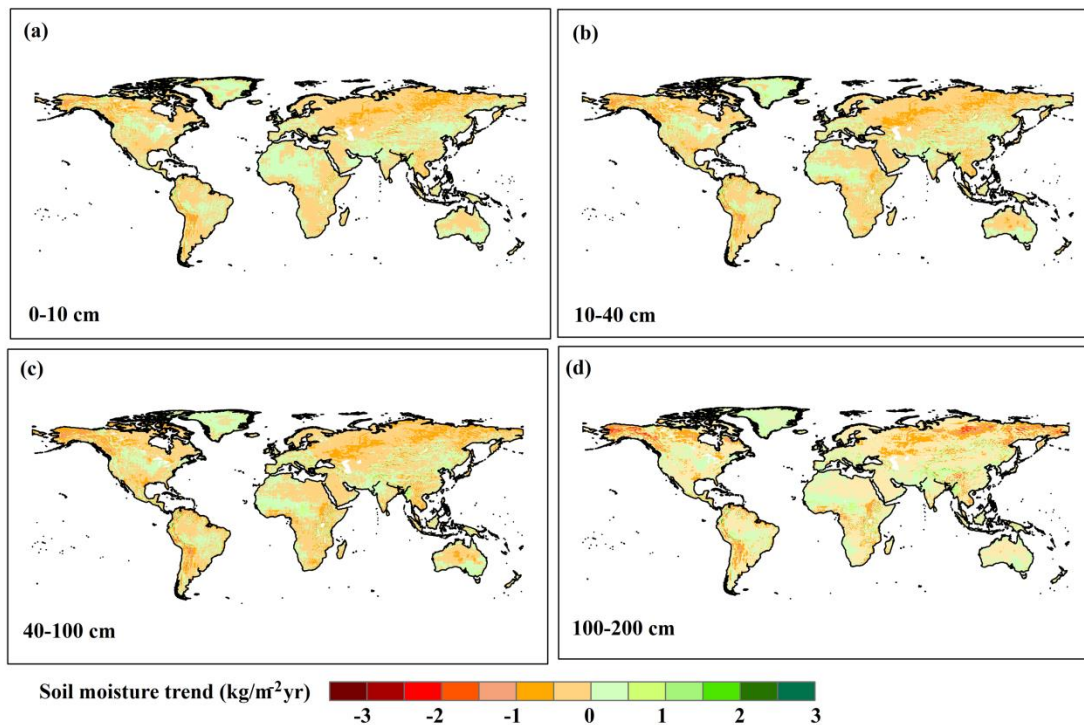


Fig. 4. (a) Spatial pattern of PET trend. (b) Partial correlations between NPP and PET.

399

400



401

402

Fig. 5. Trends of soil moisture in different layers in 2000-2014.